332 KSME Journal, Vol. 10, No. 3, pp. 332~340, 1996

A Rotordynamic Analysis of an Annular Honeycomb Seal Using a Two-Control Volume Model

T. W. HA* and D. W. Childs**

(Received March 15, 1996)

Basic equations are derived for an annular honeycomb gas seal based on a two-control volume model. The two-control volume model includes additionally a transient radial velocity component at a porous honeycomb stator surface while a conventional one-control volume model takes only the axial and the circumferential velocity components in a seal. By using a perturbation analysis and a numerical integration method, the basic equations are solved to yield the force and the corresponding dynamic coefficients developed by the seal. The two-control volume model analysis is compared to both the one-control volume model and experimental results. The comparisons show that the two-control volume analysis generally improves the predictions of rotordynamic coefficients, especially, for direct damping.

Key Words: Honey Comb Seal, Gas Seal, Rotordynamic Coefficients, Perturbation Analysis

Nomenclature

b : Honeycomb cell width (mm)
C, c : Direct and cross-coupled damping coefficients (N · s/mm)
C_e : Nominal radial clearance at seal entrance (mm)
C_x : Nominal radial clearance at seal exit (mm)
C_v : Specific heat at constant volume
d : Honeycomb cell depth (mm)
D_h : Hydraulic diameter (m)
e_h : Surface roughness height (m)
f : Fanning friction factor
F_X, F_Y : Components of seal reaction force (N)
H : Local film thickness (mm)
K, k : Direct and cross-coupled stiffness (N/mm)
L : Seal length (m)
Ma : Mach number
P : Pressure (bar)
R : Seal radius (m)
Re : Reynolds number
T : Temperature (°K)
t : Time (s)
U_s, U_r : Bulk-flow velocities relative to stator and rotor of Eq. (6)
U_z, U_θ : Fluid velocity in the axial and circumferential direction (m/s)
V : Fluid velocity in the radial direction (m/s)
X, Y : Rotor displacements from its static position (m)
ε : Eccentricity perturbation (m)
ρ : Fluid density (kg/m^3)
ω : Rotor angular velocity (rad/s)

Subscripts

a, b : Reservoir and sump
r, s : Rotor and stator
z, θ : Axial and circumferential directions
0, 1 : Zeroth and first-order perturbations

* Assistant professor, Architectural Equipment Engineering Department, Kyung-won University, Sungnam, Korea
** Professor, Mechanical Engineering Department, Turbomachinery Laboratory, Texas A & M University

1. Introduction

The forces generated within annular pressure gas seals can have a significant influence on the rotordynamics of high performance turboma-

chinery and are typically modeled by the following reaction-force/motion model:

$$-\begin{Bmatrix} F_X \\ F_Y \end{Bmatrix} = \begin{bmatrix} K & k \\ -k & K \end{bmatrix} \begin{Bmatrix} X \\ Y \end{Bmatrix} + \begin{bmatrix} C & c \\ -c & C \end{bmatrix} \begin{Bmatrix} \dot{X} \\ \dot{Y} \end{Bmatrix} \quad (1)$$

Here, X and Y define the motion of the rotor relative to the stator, F_X and F_Y are the reaction force components on the rotor and the rotordynamic coefficients K, k, C, c are the direct stiffness, cross-coupled stiffness, direct damping and cross-coupled damping coefficients, respectively.

The most popular annular seal used in current turbomachinery is the labyrinth seal, because of its good leakage control and cheap cost. However, the flow-induced forces within labyrinth seals can induce rotordynamic instability. Honeycomb seals, as shown in Fig. 1, offer an alternative to labyrinth seals. The honeycomb stator is provided to reduce leakage and has the major additional benefit of reducing the average circumferential velocity within the seal and the destabilizing cross-coupled stiffness coefficient k of Eq. (1). The honeycomb seal has been used profitably for balance-drum applications in compressors and as a turbine-interstage seal for the high-pressure oxygen turbopump (HPOTP) of the Space Shuttle Main Engine (SSME).

Several efforts have been made to theoretically predict and experimentally measure the rotordynamic characteristics of honeycomb seals. Elrod et al. (1989, 1990) tried to predict leakage and rotordynamic coefficients first by altering Nelson's (1985) basic model for honeycomb seals with two different friction-factor models. In Elrod's first analysis (1989), an entrance region friction-factor for duct flow was developed and used instead of entrance-loss coefficient. In the second analysis (1990), an empirical definition was introduced for the friction-factor variation along the seal based on measurements for a nonrotating honeycomb stator with smooth seal test apparatus. Childs et al. (1989) presented test results for seven honeycomb stators while varing cell sizes and depths and provided comparisons to results for a smooth and a labyrinth seal. Their comparisons showed that honeycomb-stator seals are more rotordynamically stable than labyrinth-stator seals. Kleynhans (1991) presented experimental results for short ($L/D=1/6$) honeycomb seals with smooth rotors. His results showed that the rotordynamic behavior of honeycomb-stator seals had erratic dependency on honeycomb cell sizes, depths and clearances. He also compared his data to theoretical predictions using Nelson's analysis with Moody friction factor model for honeycomb surfaces. This comparison was generally poor, possibly because Moody's friction-factor model for honeycomb surfaces is insufficient. To try to explain the erratic behavior of honeycomb-stator seals, Ha et al. (1991a, 1991b) developed a flat plate tester to measure the friction factors for flow between apposed parallel honeycomb surfaces. Friction-factor test results for honeycomb test surfaces showed the same erratic dependency on cell sizes, depths and clearances that rotordynamic results had shown for honeycomb seals. Ha et al. (1994) developed a rotordynamic analysis model for honeycomb-stator gas seals using an empirical friction-factor model based on flat-plate test results. Their results showed that honeycomb friction-factor model analysis provided improved predictions of leakage and rotordynamic coefficients, especially direct and cross-coupled stiffness, when compared with Moody's friction-factor model analysis. However, predictions was generally unsatisfactory when compared with Kleynhans' experimental results.

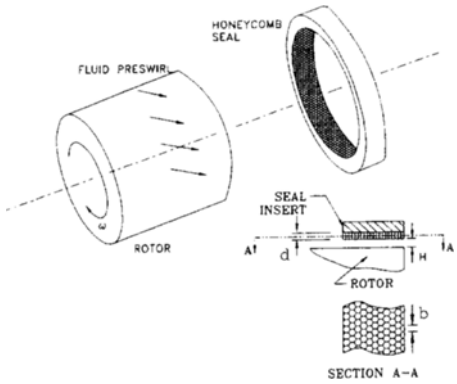

Fig. 1 Honeycomb seal geometry

The rotordynamic analysis models for honeycomb seals have developed basically from Nelson's model which used "Bulk-flow" concept for a control volume between two rigid (rotor and stator) surfaces. Because these models only account for shear stresses at the boundaries (rotor and stator) of bulk-flow model, efforts have been concentrated on defining surface friction-factor of honeycombs for improving predictions of honeycomb seals. The control volume used in honeycomb seal analysis by Ha et al (1994) has rigid surface at the rotor and a "porous" surface (honeycomb) at the stator wall. Therefore, transient radial flow is possible into or out of the porous surface (honeycomb cavity) boundary of the control volume. This situation is comparable to flow in and out of a labyrinth cavity, Scharrer (1988). The purpose of this paper is to examine predictions of rotordynamic characteristics for honeycomb seals with a two-control volume model which allows transient flow across the honeycomb surface.

2. Two-Control Volume Model

Figure 2 illustrates the basic geometry and coordinate system for the annular honeycomb seal analysis. An one-control volume model used by Ha et al. (1994) can only consider a directional velocity component (U_z) and a circumferential velocity component (U_θ) in a control volume. As noted above, the flow in the honeycomb seal may have a directional velocity component, circumferential velocity component and transient radial velocity component (V) at the honeycomb surfaces. One-control volume model is not able to take account of this situation. Comparing the analysis of labyrinth to honeycomb seals does suggest one fairly simple modification of the one-control volume model for honeycomb geometries. Two-control volume, as shown in Fig. 2, is set for present analysis. Control volume I with the seal clearance (H) is the same as the one-control volume analysis and control volume II is set inside of honeycomb cavities with cell depth (d). The compressibility and energy of the fluid within the honeycomb cavities can be modeled by control volume II.

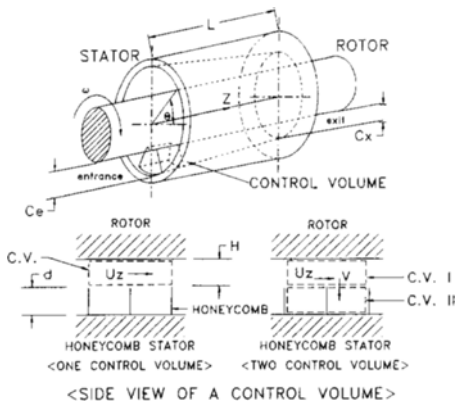

Fig. 2 Coordinates and control volumes used in analysis

3. Governing Equations

The present study extends Ha et al. (1994)'s governing equations, which used the one-control volume model, for two-control volume shown in Fig. 2 incorporating the empirical friction-factor model for the honeycomb surface and the Moody's friction-factor model for the smooth rotor surface. Governing equations can be developed for both control volume I and control volume II and finally, two equations can be combined for a simplicity. Continuity equations are written for (a) the combined control volume with depth ($H+d$) and (b) the control volume II which is within the honeycomb of depth d. The control volume equation includes the radial velocity component V of fluid entering the honeycomb. These governing continuity equations are:

Continuity A

$$\frac{\partial}{\partial t}[\rho(H+d)]+\frac{\partial(\rho U_z H)}{\partial z}+\frac{1}{R}\frac{\partial(\rho U_\theta H)}{\partial \theta}=0 \tag{2}$$

Continuity B

$$\rho V = d\frac{\partial \rho}{\partial t} \tag{3}$$

After reduction by these continuity equations, The one-control volume momentum equations are unchanged for the two-control volume momen-

tum equations. Beyond its use in reduction of the momentum equations, the second continuity equation does not enter the model.

Axial-Momentum

$$-H\frac{\partial P}{\partial Z}=\frac{\rho}{2}U_zU_sf_s+\frac{\rho}{2}U_zU_rf_r+\rho H\frac{D(U_z)}{Dt} \tag{4}$$

Circumferential-Momentum

$$-\frac{H}{R}\frac{\partial P}{\partial \theta}=\frac{\rho}{2}U_\theta U_sf_s+\frac{\rho}{2}(U_\theta-R\omega)U_rf_r+\rho H\frac{D(U_\theta)}{Dt} \tag{5}$$

where, U_z and U_θ are the bulk-flow velocities relative to the wall and defined as

$$U_s=(U_z^2+U_\theta^2)^{1/2}$$
$$U_r=[U_z^2+(U_\theta-R\omega)^2]^{1/2}$$
$$\frac{D}{Dt}=\frac{\partial}{\partial t}+\frac{U_\theta}{R}\frac{\partial}{\partial \theta}+U_z\frac{\partial}{\partial Z} \tag{6}$$

f_s and f_r are the stator (honeycomb) and rotor (smooth) surface friction factors defined as

$$f_r=0.001375\left[1+\left(20000\frac{e_h}{D_h}+\frac{10^6}{Re}\right)^{1/3}\right]$$
$$f_s=c_1+\frac{H}{b}\left(\frac{c_2}{\left(\frac{P}{P_c}\right)}+c_3(Ma)^{c_4}\right) \tag{7}$$

Where, e_h is the absolute roughness of the surface, D_h is the hydraulic diameter, Re is the Reynolds number, Ma is the Mach number, P_c the critical pressure of air (37.7 bar) and c_1-c_4 are constants listed in Table 1 of Ha et al. (1994).

The energy equation for the combined control volume is:

Energy

$$\rho H\frac{De}{Dt}+\rho d\frac{\partial e}{\partial t}+\frac{\partial(PU_zH)}{\partial Z}+\frac{1}{R}\frac{\partial(PU_\theta H)}{\partial \theta}=\frac{\rho f_rR\omega(R\omega-U_\theta)}{2} \tag{8}$$

Where

$$e=C_vT+\frac{(U_\theta^2+U_z^2)}{2} \tag{9}$$

is the internal energy per unit mass, C_v is the specific heat at constant volume and T is the temperature. For $d=V=0$, these governing equations reduce to the one-control volume analysis.

4. Solution Procedure

Basically the solution procedure of governing equations is the same as Ha et al. (1994) For small motion of the rotor about its geometric center, the pressure, density, axial velocity, circumferential velocity and local seal clearance can be expanded in terms of zeroth-order and first-order perturbation variables.

$$P=P_0+\varepsilon P_1$$
$$\rho=\rho_0+\varepsilon\rho_1$$
$$U_z=U_{z0}+\varepsilon U_{z1}$$
$$U_\theta=U_{\theta0}+\varepsilon U_{\theta1}$$
$$H=H_0+\varepsilon H_1 \tag{10}$$

Substitution of these perturbed variable into governing Eqs. (2)~(5) and (8) yields a set of zeroth-order and first-order equations. The nonlinear zeroth-order equations are numerically integrated using a Runge-Kutta method to obtain matched boundary conditions which are detailed in Ha et al. (1994). A seperation-of-variable solution approach is used for the first-order perturbation equations. By assuming a circular precessional seal motion, the time dependency in the governing equations is eliminated. A transition-matrix approach, Meirovitch (1985), is used to solve the first-order perturbation equations. The first-order pressure solution is then integrated axially and circumferentially to determine the rotordynamic coefficients in Eq. (1).

5. Results

This section illustrates the validity of the two-control volume model analysis in predicting the rotordynamic characteristics of annular honeycomb stator gas seals. To show the improvement in predition, the two-control volume analysis is compared with the one-control volume model analysis of Ha et al. (1994) and also compared with experimental test results taken by Kleynhans (1991). In the two-control volume model, honeycomb cell depth (d) is an added parameter compared with the one-control volume model. The effect of cell depths for the rotordynamic

coefficients will be also presented. The two-control volume model includes the radial velocity component V as well as the axial and the circumferential velocity components. However, the radial velocity component does not affect to leakage. Therefore, the leakage result of the two-control volume model is the same as the one-control volume model's result and only dynamic results will be discussed in this study.

The geometry and operating conditions for the seals used in the example are given as follow :

Geometry :

(1) Seal length(L) : 25.4 mm

(2) Rotor diameter(D) : 152.4 mm

(3) Seal clearance(H) : 0.41 mm

(4) Stator geometry : Honeycomb stator(b=0.79 mm, d=2.29 mm)

(5) Rotor geometry : Smooth rotor(effective roughness=8.128×10^{4} mm)

Operating conditions :

(6) Reservoir pressure(Pa) : 7.9 bar

(7) Pressure ratio(Pb/Pa) : 0.56, 0.45 and 0.4

(8) Reservoir temperature(T) : 300°K

(9) Preswirl ratio($U_{\theta0}(0)/R\omega$) : 0.0~1.2(= inlet circumferential velocity ratio)

(10) Shaft speed(ω) : 5000, 12,000 and 16,000 rpm

5.1 Direct stiffness

In general, the direct stiffness of a gas seal does not directly influence the rotordynamic instability of the rotor. However, if sufficiently large, it can increase the critical speed. Fig. 3 shows direct stiffness versus inlet circumferential-velocity ratio with pressure ratio as a parameter. The two-control volume model analysis (dotted line) predicts direct stiffness slightly better than the one-control volume model analysis. This implies that the consideration of the transient radial velocity component does not affect much to the radial force component of the rotor. Theoretical predictions are generally poor, specially for the high pressure ratio.

5.2 Cross-coupled stiffness

The tangental component of seal's rotordynamic force acting on the rotor which is precessing in the direction of rotation is represented by the cross-coupled stiffness. A positive cross-coupled stiffness increases the forward precessing motion has a destabilising effect and the cross-coupled stiffness depends on the magnitude and direction (with respect to rotor rotation) of the circumferential velocity of the fluid within the seal. The transient radial velocity component may disturb the development of circumferental velocity due to the rotation of the rotor. Therefore, the two-control volume model which includes the radial velocity component may yields lower cross-coupled stiffness than the model of neglect-

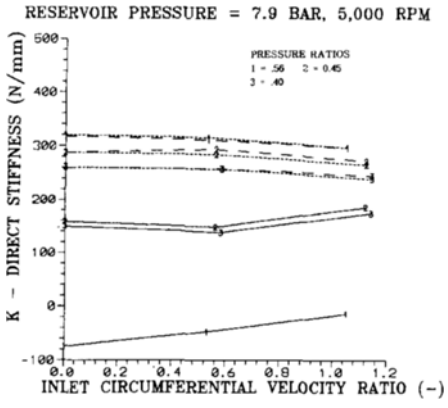

Fig. 3 Direct stiffness versus inlet circumferential velocity ratio ; experimental (solid), two-control volume model (dotted), one-control volume model (dashed)

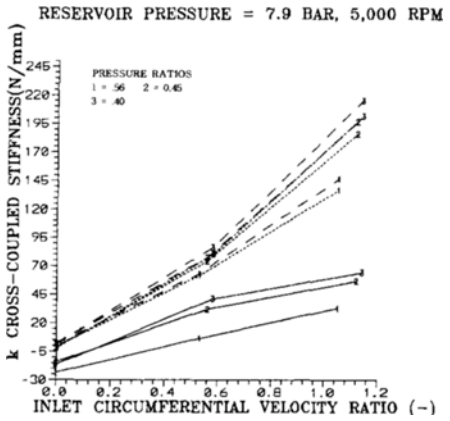

Fig. 4 Cross-coupled stiffness versus inlet circumferential velocity ratio ; experimental (solid), two-control volume model (dotted), one-control volume model (dashed)

ing the radial velocity (the one-control volume model). Fig. 4 shows that the two-control volume model (dotted line) predicts the cross-coupled stiffness lower than the one-control volume model (dashed line) and illustrates better predictions. However, there is still a major difference between the theoretical predictions and experimental measurements (solid lines).

5.3 Direct damping

The direct damping represents the tangential component of the seal's rotor dynamic force which opposes the precessional motion and has a stabilizing effect. The direct damping may also relate to the circumferential velocity component of the flow within the seal. The consideration of the transient radial velocity yields much improvement in the preditions of the direct damping. Figs. 5~7 shows the direct damping versus inlet circumferential velocity ratio with pressure ratio as a parameter for 5000, 12000 and 16000 rpm, respectively. The two-control volume model analysis (dotted line) yields lower value of the direct damping coefficient than the one-control volume model analysis (dashed line) to be closer to the experimental result (solid line). The improvement of the direct damping predition becomes better as increasing the rotor speed. For the rotor speed of 16000 rpm, the two-control volume model analysis yields very close to the experimental results as shown in Fig. 7. However, the trend for pressure ratios does not show a good agreement between the theoretical predition and the experimental measurement.

5.4 Whirl frequency ratio

The whirl frequency ratio, $k/\omega C$, is a ratio of the destabilizing forces to the stabilizing forces and should be minimized, if possible. The two-control volume model (dotted line) yields slightly higher value of the whirl frequency ratio than the one-control volume model (dashed line) as shown

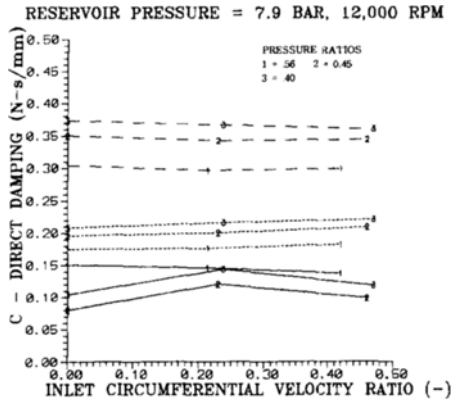

Fig. 5 Direct damping versus inlet circumferential velocity ratio for 5000 rpm; experimental (solid), two-control volume model (dotted), one-control volume model (dashed)

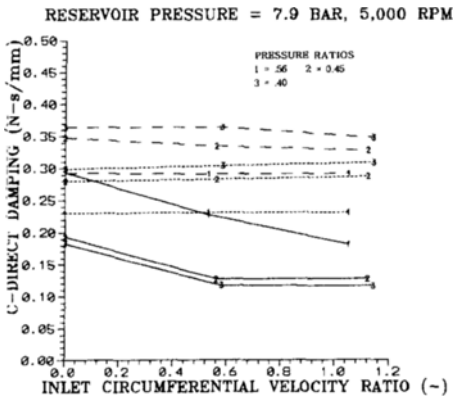

Fig. 6 Direct damping versus inlet circumferential velocity ratio for 12,000 rpm; experimental (solid), two-control volume model (dotted), one-control volume model (dashed)

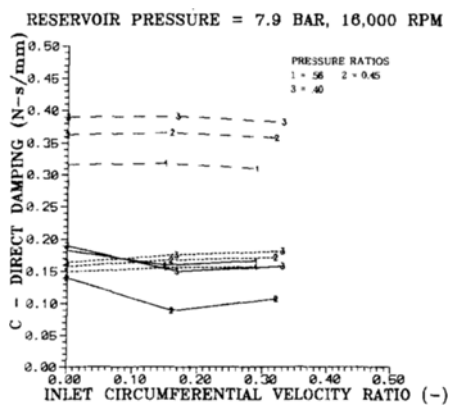

Fig. 7 Direct damping versus inlet circumferential velocity ratio for 16,000 rpm; experimental (solid), two-control volume model (dotted), one-control volume model (dashed)

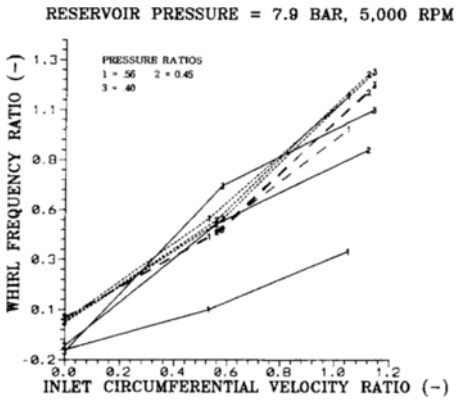

Fig. 8 Whirl frequency ratio versus inlet circumferential velocity ratio; experimental (solid), two-control volume model (dotted), one-control volume model (dashed)

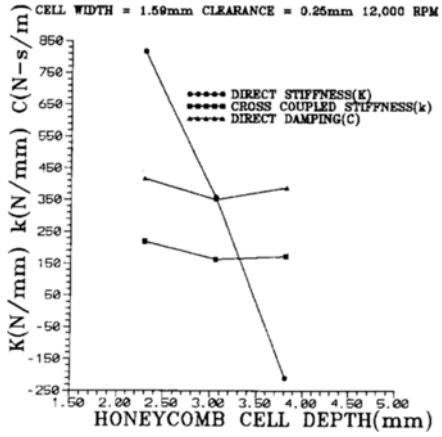

Fig. 9 Rotordynamic coefficients versus honeycomb cell depth

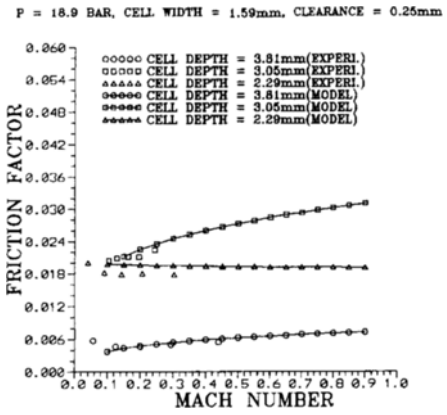

Fig. 10 Friction factor characteristics of the honeycomb surface

in Fig. 8. The two-control volume model improves the predition of the whirl frequency ratio for low inlet circumferential velocity cases with low pressure ratios comparing to the experimental results (solid line) in Fig. 8.

5.5 Effect of honeycomb cell depth (d)

The two-control volume model has the additional parameter of the cell depth (d) as shown in Eqs. (2),(3) and (8), comparing to the one-control volume model. The control volume II (see Fig. 2) is set with the honeycomb cell depth in order to considering the transient radial velocity component within the honeycomb cell. It may be valuable to see the effect of the honeycomb cell depth for the honeycomb seal's rotordynamic characteristics. Since the honeycomb cell depth is very closely related to the surface friction factor of the honeycomb (Ha et al.(1992a), it is needed to see the rotordynamic effect of cell depth relating with the friction factor characteristic of cell depth. Only three cell depth (2.29 mm, 3.05 mm and 3.81 mm) data are available in this study. Figure 9 shows the effect of honeycomb cell depth for direct stiffness, closs-coupled stiffness and direct damping in the case of 1.59 mm honeycomb cell width, 0.25 mm clearance, 12,000 rpm and Reynolds number 50,000(Ma=0.45). Figure 10 shows the experimental and the model data(f_r in Eq. (7)) of the honeycomb surface friction factor for 1.59 mm cell width with 0.25 mm clearance case. As shown in Fig. 10, the friction factor of 3.05 mm cell depth case is the biggest and follows by 2.29 mm and 3.81 mm case for the Mach number of 0.45 flow condition. The direct stiffness is sharply decreased as increasing the cell depth as shown in Fig. 9. A possible explanation is that increasing the cell depth means increasing the effective clearance to yield lower value of the direct stiffness. The cross-coupled stiffness and the direct damping show different trend from the direct stiffness as shown in Fig. 9. The cross-coupled stiffness and the direct damping are decreasing and then increasing as increasing the cell depth. The comparison of the friction factor

characteristic shows that increasing the friction factor yields decreasing the k and C and oppositely decreasing the friction factor yields increasing the k and C. This means that k and C are sensitive to the characteristics of the friction factor with cell depths which affect the development of circumferential flow in the seal.

6. Conclusions

To improve the theoretical analysis of rotordynamic characteristics of an annular honeycomb gas seal, the two-control volume model which takes account of the additional transient radial flow component as well as the directional and the circumferential velocity components has been developed. The two-control volume model analysis has been compared with the one-control volume model which includs only the directional and the circumferential velocity components in a honeycomb seal and also compared with experimental results to show the improvement in predictions. The results presented support the following conclusions.

(1) The two-control volume analysis does not change leakage results compared to the one-control volume analysis.

(2) The two-control volume analysis predicts the direct stiffness slightly better than the one-control Volume model one. This implies that a consideration of the transient radial velocity does not much affect to the radial force component of the rotor.

(3) For the cross-coupled stiffness, the two-control volume model analysis provides lower value to be better predictions than the one-control volume model analysis.

(4) The two-control volume model analysis illustrates the best improvement in the direct damping predictions. As increasing the rotor speed, the improvement of the direct damping prediction becomes better to yield very close to the experimental results at 16000 rpm.

(5) For the effect of honeycomb cell depths on the rotordynamic characteristics, the direct stiffness is sharply decreasing as increasing the cell depths. However, the cross-coupled stiffness and the direct damping are sensitive to the characteristics of the friction factor with cell depths. For the case of increasing a friction factor as increasing a cell depth, k and C turn out to be decreased, and vice versa.

References

Childs, D. W., Elrod, D. and Hale, K., 1989, "Annular Honeycomb Seals: Test Results for Leakage and Rotordynamic Coefficients; Comparisons to Labyrinth and Smooth Configurations," *ASME Journal of Tribology*, Vol. 111, Apr., pp. 293~301.

Elrod, D., Nelson, C. and Childs, D. W., 1989, "An Entrance Region Friction Factor Model Applied to Annular Seal Analysis: Theory Versus Experiment for Smooth and Honeycomb Seals," *ASME Journal of Tribology*, Vol. 111, Apr., pp. 337~343.

Elrod, D., Childs D. W. and Nelson C. C., 1990, "An Annular Gas Seal Analysis Using Empirical Entrance and Exit Region Friction Factors," *ASME Journal of Tribology*, Vol. 112, Apr., pp. 196~204.

Ha, T. W. and Childs, D. W., 1992a, "Friction-Factor Data for Flat Plate Tests of Smooth and Honeycomb Surfaces," *ASME Journal of Tribology*, Vol. 114, Oct., pp. 722~730.

Ha, T. W., Morrison, G. L. and Childs, D. W., 1992b, "Friction-Factor Characteristics for Narrow Channels with Honeycomb Surfaces," *ASME Journal of Tribology*, Vol. 114, Oct., pp. 714~721.

Ha, T. W. and Childs, D. W., 1994, "Annular Honeycomb-Stator Turbulent Gas Seal Analysis Using a New Friction-Factor Model Based on Flat Plate Tests", *ASME Journal of Tribology*, Vol. 116, Apr., pp. 352~360.

Kleynhans, G. F., 1991, "A Comparison of Experimental Results and Theoretical Predictions for the Rotordynamic and Leakage Characteristics of Short(L/D=1/6) Honeycomb and Smooth Annular Pressure Seals," Master thesis, Texas A & M University, College Station, TX.

Meirovitch, L., 1985, *Introduction to Dynamics and Control*, Wiley, New York, NY.

Nelson, C. C., 1985, "Rotordynamic Coefficients for Compressible Flow in Tapered Annular Seals," *ASME Journal of Tribology*, Vol. 107, No. 3, pp. 318~325.

Scharrer, J. K., 1988, "Theoy Versus Experiment for the Rotordynamic Corfficients of Labyrinth Gas Seals: Part 1-A Two-Control-Volume Model," *ASME Journal of Vibrations*, Acoustics, Stress and Reliability in Design, Vol. 110, No. 3, July, pp. 270~280.